Monatshefte für Chemie 129, 455–466 (1998)

Monatshefte für Chemie
Chemical Monthly

Printed in Austria

Synthesis and Characterization of Some Transition Metal Complexes of 2-Amino-3-hydroxypyridine and its Application in Corrosion Inhibition

S. I. Mostafa[1,*] and **S. A. Abd El-Maksoud**[2]

[1] Chemistry Department, Faculty of Science, Mansoura University, Mansoura, Egypt
[2] Chemistry Department, Faculty of Education, Suez Canal University, El-Arish, Sinai, Egypt

Summary. The new complexes *cis*-$Mo_2O_5(ahp)_2$, *trans*-$UO_2(ahp)_2$, $ReO(PPh_3)(ahp)_2I$, $M(ahp)_2$, and $M'(ahp)_3$ (M = Co, Cu, Pd; M' = Fe, Ru, Rh; *ahp* = 2-amino-3-hydroxypyridine) have been prepared. The ligand binds *via* the deprotonated hydroxy oxygen atom and the amino nitrogen atom to the central ion. Infrared, *Raman*, ^{1}H NMR, and electronic spectra of the complexes have been recorded. 2-Amino-3-hydroxy pyridine was found to behave as an inhibitor with respect to the corrosion of aluminum and copper in acidic solutions.

Keywords. Complexes; Copper; Transition metal; Corrosion inhibition.

Synthese und Charakterisierung einiger Übergangsmetallkomplexe von 2-Amino-3-hydroxypyridin sowie dessen Anwendung als Korrosionshemmer

Zusammenfassung. Die neuen Komplexe *cis*-$Mo_2O_5(ahp)_2$, trans-$UO_2(ahp)_2$, $ReO(PPh_3)(ahp)_2I$, $M(ahp)_2$ und $M'(ahp)_3$ (M = Co, Cu, Pd; M' = Fe, Ru, Rh; *ahp* = 2-Amino-3-hydroxypyridin) wurden hergestellt. Die Liganden binden über den deprotonierten Hydroxylsauerstoff und den Aminstickstoff an das Zentralatom. Infrarot-, *Raman*-, UV- und ^{1}H-NMR-Spektren der Verbindungen wurden aufgenommen. 2-Amino-3-hydroxypyrimidin wirkt als Korrosionshemmer für Aluminium und Kupfer in sauren Lösungen.

Introduction

2-Amino-3-hydroxypyridine (H*ahp*, Fig. 1; H is the dissociable hydroxy proton) is of interest since its anion chelates metal ions as a bidentate N,O donor forming five membered rings like that of 2-aminophenol [1, 2] (Fig. 2). 2-Amino-3-hydroxypyridine is biologically important in the preparation of clinical antiinflammatory analgesics [3]. There are only few known transition metal complexes [4,5] or crystal structures [6] of 2-amino-3-hydroxypyridine: $[Cp_2Zr(ahp)]^+$ [4], $[RuCl_2(AsPh_3)_2(ahp)]$ [5], and $[(abhp)_2Cu_2Br_6 \cdot 2H_2O]$ ([6]; *abhp* = 2-amino-4-

* Corresponding author

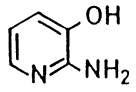

Fig. 1. 2-Amino-3-hydroxypyridine

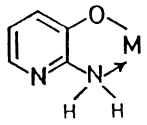

Fig. 2. Five-membered ring formed by chelation of 2-amino-3-hydroxypyridine with a metal ion

bromo-3-hydroxypyridine). Also, the complexes of 2-amino-3-hydroxypyridine-salicylaldehyde *Schiff* base with *M*(II) (Co, Ni, Cu, Pt) and VO^{2+} have been reported [7]. The most efficient acid inhibitors in cleaning solution for industrial equipment are organic compounds containing nitrogen and sulfur atoms and contain multiple bonds through which they are adsorbed on the metal surfaces. Hydrazines [8], substituted hydrazines [9], ethyl amine [10], substituted phenols [11], and hydrazones [12] have been reported as effective corrosion inhibitors for aluminum and copper.

Here we report the synthesis of new complexes of 2-amino-3-hydroxypyridine with a number of transition elements and their vibrational, ^{1}H NMR, and electronic spectra. The inhibition behaviour of 2-amino-3-hydroxypyridine towards the corrosion of aluminum and copper in acidic solutions have been studied as well.

Results and Discussion

Preparations

The molybdenum oxo complex *cis*-$Mo_2O_5(ahp)_2$ was obtained by addition of ammonium molybdate to 2-amino-3-hydroxypyridine in aqueous solution. *Trans*-$UO_2(ahp)_2$ was formed by reaction of uranyl acetate and the ligand in aqueous methanolic solution. The complex $ReO(PPh_3)(ahp)_2I$ was synthesized by mixing $ReO_2(PPh_3)_2I$ and the ligand in methanol. The *tris*-*M*$(ahp)_3$(*M* = Fe, Ru, Rh) complexes were obtained by reaction of the hydrated metal chloride with the ligand in methanolic (Ru) or basic aqueous (Fe, Rh) solutions. The palladium complex $Pd(ahp)_2$ was prepared from an aqueous solution of $K_2[PdCl_4]$ and the ligand, whereas *M*$(ahp)_2$(*M* = Co, Cu) complexes were formed from the hydrated metal acetate and the ligand in methanol.

Vibrational spectra

Infrared and Raman spectroscopic data for the free ligand and its complexes are shown in Table 1. The stretching vibration of the free ligand (ν(OH), 3250 cm^{-1}) is not observed in the complexes, suggesting deprotonation of the hydroxy group and formation of M-O bonds [4,13]. Bands near 3440 and 3310 cm^{-1} in the free ligand are assigned to $\nu_{asym}(NH_2)$ and $\nu_{sym}(NH_2)$, respectively; these bands are shifted to lower wave numbers in the complexes due to the coordination of the amino group

nitrogen atom to the metal ion [4]. The strong band at 1600 cm^{-1} assigned to $\delta(NH_2)$ in the ligand is shifted near 1620 cm^{-1} in the complexes [5]. In the spectra of ligand and complexes, the bands observed near 1290 and 1210 cm^{-1} probably arise from ν(C-N) and ν(C-O) stretching vibrations, respectively [4, 5, 13].

In *cis*-$Mo_2O_5(ahp)_2$, the symmetric stretch $\nu_{sym}(MO_2)$ is observed at 960 cm^{-1} as a strong band in the *Raman* spectrum, and as a weaker band at 980 cm^{-1} in the IR spectrum. $\nu_{asym}(MO_2)$ values (IR, 906 cm^{-1}, strong; *Raman*, 880 cm^{-1}, weak) are close to those observed for reported complexes containing the *cis*-MoO_2 moiety [14]. Also, the IR spectrum of *cis*-$Mo_2O_5(ahp)_2$ shows a broad band at 700 cm^{-1} assigned to $\nu(Mo_2O)$ of the bridging oxo ligand [13, 15]. The *trans*-$UO_2(ahp)_2$ complex has a strong IR band at 902 cm^{-1} not observable in the *Raman* spectrum assigned to $\nu_{asym}(UO_2)$ of the *trans*-O = U = O moiety [13, 16], whereas the strong *Raman* band at 890 cm^{-1} is assigned to $\nu_{sym}(UO_2)$ [13]. The complex $ReO(PPh_3)(ahp)_2)I$ shows a new strong band at 967 cm^{-1} (IR) and 983 cm^{-1} (*Raman*) which arises from the ν(ReO) stretch [17]. The complexes $M(ahp)_2$ (M = Co, Cu, Pd) show a new band near 500 cm^{-1} in both the IR and *Raman* spectra which may arise from ν(M-O) stretches [18,19]. New bands can be been found near 470 cm^{-1} in the IR and *Raman* spectra of all reported complexes, probably arising from $\nu(M\text{-N})$ modes [4, 5, 20, 21].

^{1}H NMR spectra

The ^{1}H NMR spectroscopic data for 2-amino-3-hydroxypyridine and its complexes $Mo_2O_5(ahp)_2$, $Rh(ahp)_3$, and $Pd(ahp)_2$ in *DMSO*-d_6 are given in Table 1. The ^{1}H NMR spectrum of the free ligand shows a triplet at $\delta = 6.39$ ppm and two doublets at $\delta = 6.81$ and 7.40 ppm, arising from H_5, H_4, and H_6 respectively (see Fig. 1 for numbering scheme). The protons of the hydroxy and amino groups appear as singlets at $\delta = 9.47$ (broad) and 5.41 ppm, respectively. For the complexes, the resonance arising from the hydroxy proton disappears, whereas that arising from the amino protons is shifted to lower field indicating chelation of the ligand *via* the deprotonated hydroxy oxygen atom and the amino nitrogen atom to the metal ion [4]. Also, the resonances arising from H_4, H_5, and H_6 are shifted to higher field, probably due to electron withdrawal by the metal causing decreased electronic density in the pyridine ring [22].

The ^{1}H NMR spectrum of *cis*-$Mo_2O_5(ahp)_2$ (Fig. 3) reveals the presence of two isomeric products *A* and *B* in a ratio of approximately 4:1, with most of the minor isomer peaks downfield from the major isomer counterpart. In the major isomer *A*, the amino group nitrogen atoms attached to C_2 and C_2' are *trans* to the molybdenum oxo ligand [23] as shown in Fig. 4a. This feature is supported by the X-ray crystal structure of $[MoO_2(Hamp)_2]$ [1], $[MoO_2(trop)_2]$ [24], and $[MoO_2(2,3\text{-}dhb)_2]$ [25]. In the minor isomer *B*, the oxygen atom attached to C_3' and the nitrogen atom attached to C_2 are *trans* to the molybdenum oxo ligand (Fig. 4b). The first isomer has three further resonances corresponding to the protons of isomer *B* [20]. The triplet resonances observed at 6.29 and 6.64 ppm arise from H_5 and H_5', respectively; the doublets at 6.66, 7.11, 6.38, and 7.37 ppm are due to H_4 and H_4', H_6, and H_6', respectively.

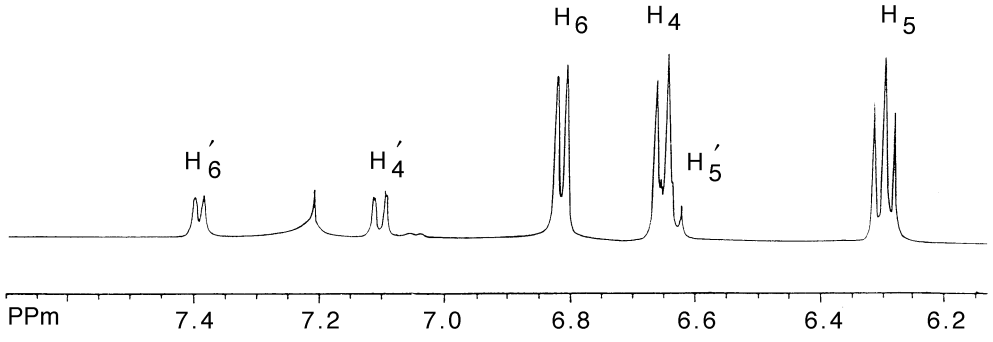

Fig. 3. ^{1}H NMR spectrum of *cis*-$Mo_2O_5(ahp)_2$

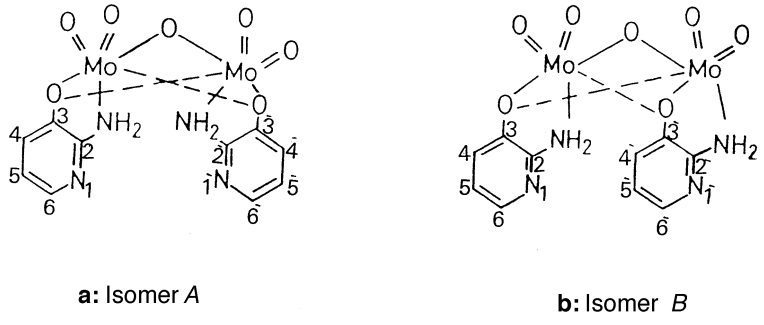

a: Isomer *A* **b:** Isomer *B*

Fig. 4. Expected isomers (*A*, *B*) of *cis*-$Mo_2O_5(ahp)_2$

Electronic spectra and magnetic studies

Electronic spectroscopic data in dimethyl sulfoxide and magnetic moments for $M(ahp)_2$ (M = Co, Cu) and $M'(ahp)_3$ (M' = Fe, Ru) are given in Table 1.

The electronic spectrum of $Co(ahp)_2$ shows two bands at 600 and 495 nm which may be assigned to $^4T_{1g}\rightarrow{}^4A_{2g}$ and $^4T_{1g}\rightarrow{}^4T_{1g}(P)$, respectively, similar to those reported in octahedral structures [26, 27]. The magnetic moment of $Co(ahp)_2$ is 3.6 BM, close to the spin-only value for octahedral Co(II) complexes [28, 29].

The electronic spectrum of $Cu(ahp)_2$ shows two absorption bands, one at 556 nm (broad) and the other one at 410 nm, which are characteristic of a square-planar structure [30, 31]. The magnetic moment value of 1.78 BM confirms the square planar geometry for Cu(II) (d^9 electronic configuration with one unpaired electron) [32]. In the electronic spectrum of $Ru(ahp)_3$, two bands are observed at 560 and 430 nm which may arise from $^2T_{2g}\rightarrow{}^2T_{2g}$, ^2E_g and $^2T_{2g}\rightarrow{}^2T_{1g}$, $^2A_{1g}$ transitions, respectively [21, 33]. The magnetic moment for $Ru(ahp)_3$ (1.8 BM) is lower than the normal value (2.1 BM), may be due to the low symmetry of the ligand field around the metal ion [34, 35]. The complex $Fe(ahp)_3$ is found to be paramagnetic with $\mu_{eff} = 2.2$ BM which may indicate a low spin ground state of the iron (III) complex [21, 36].

Table 1. Analytical, vibrational, ^{1}H NMR, and electronic spectroscopic and magnetic moment data for 2-amino-3-hydroxypyridine and its complexes

	Analysis(%)[a]			Vibrational spectra (cm^{-1})[b]							H^{1}NMR data(δ)[e]				Electronic Spectra (nm)[g]	μ_{eff} (BM)
	C	H	N	$\nu_{asym}(NH_2)$	$\nu_{sym}(NH_2)$	ν(C-N)	ν(C-O)	$\nu_{sym}(MO_2)$	$\nu_{asym}(MO_2)$	ν(*M*-N)	NH_2 (s)	H_4 (d)	H_5 (t)	H_6 (d)		
H*ahp*				3441 s *3344 m*	3314 s	1290 vs	1220 s				5.41	6.81	6.39	7.40		
cis-$Mo_2O_5(ahp)_2 \cdot 3H_2O$	21.8	2.6	10.0	3248 s	3104 s	1289 s	1210 s	980 m	906 vs	490 m	8.62[f]	6.66[f]	6.29[f]	6.83[f]		
	(22.0)	(2.9)	(10.3)					*960 s*	*880 m*		7.22	7.11	6.64	7.37		
trans-$UO_2(ahp)_2$	25.0	2.0	11.1	3341 s	3175 s	1301 vs	1210 m		902 vs	505 s						
	(24.6)	(2.05)	(11.5)					*890 s*		538 m						
$ReO(PPh_3(ahp)_2I$	41.4	3.2	6.8	3248 s	3188 s	1350 s	1260 s	967 s[c]								
	(41.5)	(3.1)	(6.9)		*3070 s*	*1360 s*	*1250 s*	*983 s*[c]								
$Fe(ahp)_3 \cdot 3H_2O$	41.1	4.6	18.8	3331 s	3108 s	1288 s	1206 m			471 s						2.2
	(41.2)	(4.8)	(19.2)													
$Ru(ahp)_3 \cdot 3H_2O$	37.3	4.5	17.3	3381 s	3185 s	1293 s	1244 s			436 m					560, 430	1.8
	(37.3)	(4.3)	(17.4)				*1220 s*			*450 s*						
$Rh(ahp)_3 \cdot 4H_2O$	35.7	4.2	16.3		3107 s	1280 s	1236 s				8.98	6.61	6.25	6.87		
	(35.9)	(4.3)	(16.7)													
$Co(ahp)_2 \cdot 2H_2O$	38.8	4.6	17.7	3396 s		1286 s	1200 m								600, 495	3.6
	(38.3)	(4.5)	(17.9)							461 s						
$Cu(ahp)_2$	42.4	3.3	19.9	3331 s		1290 s	1244 m	520 m[d]		440 m					556, 410	1.78
	(42.6)	(3.6)	(19.9)					*539 s*[d]		*450 s*						
$Pd(ahp)_2$	36.7	2.8	17.0	3237 s	3194 s	1295 s	1234 s			390 s	10.41	6.73	6.36	6.88		
	(37.0)	(3.1)	(17.3)				*1208 s*	*500 s*[d]								

[a] Calculated values in parentheses; [b] *Raman* data in italics; [c] $\nu(Re=O)$; [d] ν(M-O); [e] spectra in *DMSO*-d_6; [f] peaks due to isomer; [g] electronic spectra in $(CH_3)_2SO$

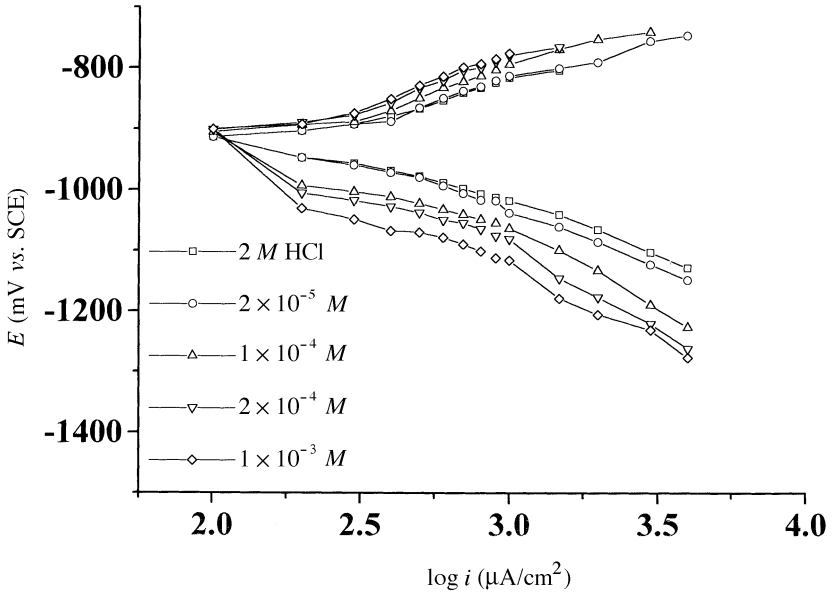

Fig. 5. Galvanostatic polarization of aluminum in 2 *M* HCl in the absence and presence of different concentrations of 2-amino-3-hydroxypyridine at 303 K

Polarization and weight loss measurements

Polarization of aluminum and copper was carried out under galvanostatic conditions in 2 *M* HCl and 2 *M* HNO_3, respectively, in the absence and presence of different concentrations of 2-amino-3-hydroxypyridine as shown in Fig. 5 and 6. Tables 2 and 3 show the effect of inhibitor concentration on the corrosion potential (E_{corr}), *Tafel* slope (B_a, B_c), corrosion current density (i_{corr}), and the degree of percentage inhibition for aluminium and copper, respectively. The inhibition efficiencies (*%P*) were calculated using the equation

$$\%P = 100(i_{corr} - i^{\alpha}_{corr})/i_{corr}$$

where i_{corr} and i^{α}_{corr} are the corrosion current density in the absence and presence of the inhibitor.

Figures 7 and 8 show the weight loss ($mg \cdot cm^{-2}$) *vs.* time of immersion relationship for aluminum in 2 *M* HCl and copper in 2 *M* HNO_3, respectively, indicating that at increasing inhibitor concentration the corrosion rate decreases. Tables 4 and 5 show the inhibition effeciency values obtained from the weight loss measurements in the presence of different concentrations of the inhibitor. The inhibition percentage (*%P*) is calculated by the equation

$$\%P = 100(W_1 - W_2)/W_1$$

where W_1 and W_2 are the weight loss in the absence and presence of the inhibitor, respectively.

From the polarization and weight loss measurements, it is evident that 2-amino-3-hydroxypyridine is an effective inhibitor of the corrosion of aluminum and copper in acidic solutions. The corrosion rate was found to decrease with increas-

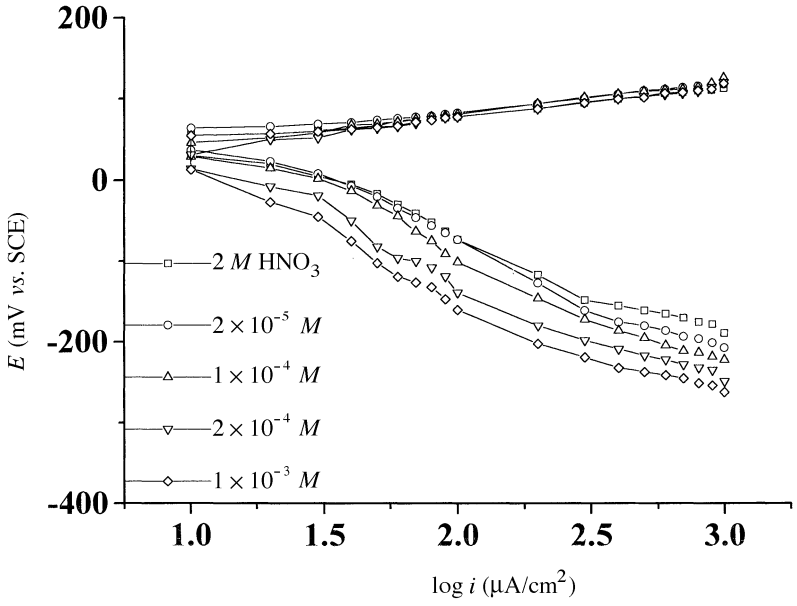

Fig. 6. Galvanostatic polarization of copper in 2 *M* HNO_3 in the absence and presence of different concentrations of 2-amino-3-hydroxypyridine at 303 K

Table 2. The effect of inhibitor concentration on corrosion current density, *Tafel* slopes, and percentage inhibition for aluminum in 2 *M* HCl at 303 K

Conc. ($mol \cdot l^{-1}$)	E^o (mV)	i_{corr} ($\mu A/cm^2$)	B_c (mV/decade)	B_a (mV/decade)	Inhibition (%)
0.0	931	252.5	149	152	–
2×10^{-5}	931	216.2	165	155	14.4
1×10^{-4}	936	149.3	167	164	40.9
2×10^{-4}	940	122.2	170	169	51.6
1×10^{-3}	942	95.1	171	169	62.3

Table 3. The effect of inhibitor concentration on corrosion current density, *Tafel* slopes, and percentage inhibition for copper in 2 *M* HNO_3; at 303 K

Conc. ($mol \cdot l^{-1}$)	E^o (mV)	i_{corr} ($\mu A/cm^2$)	B_c (mV/decade)	B_a (mV/decade)	Inhibition (%)
0.0	52	20.3	170	36	–
2×10^{-5}	56	17.0	166	37	16.2
1×10^{-4}	46	13.9	171	38	31.3
2×10^{-4}	45	9.6	177	40	52.9
1×10^{-3}	42	7.7	174	40	62.2

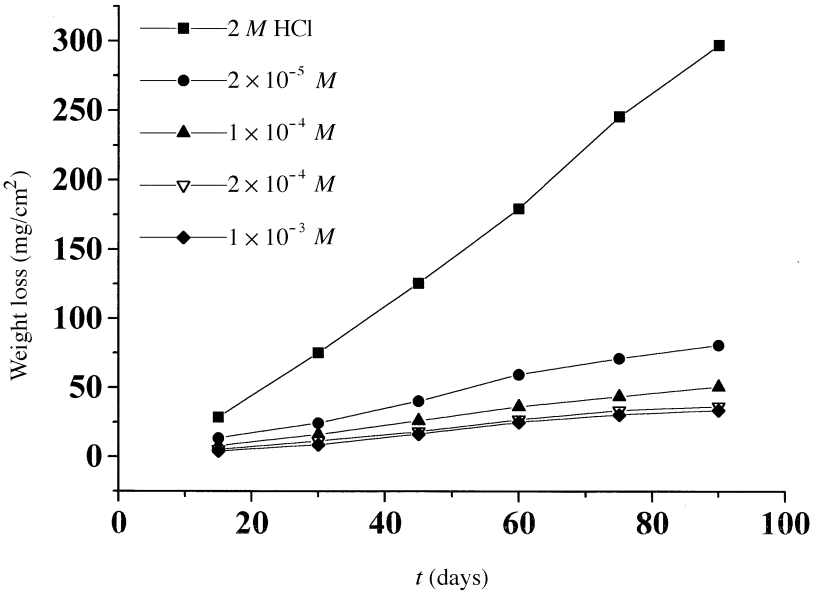

Fig. 7. Weight loss *vs* time curves of aluminum in 2 *M* HCl

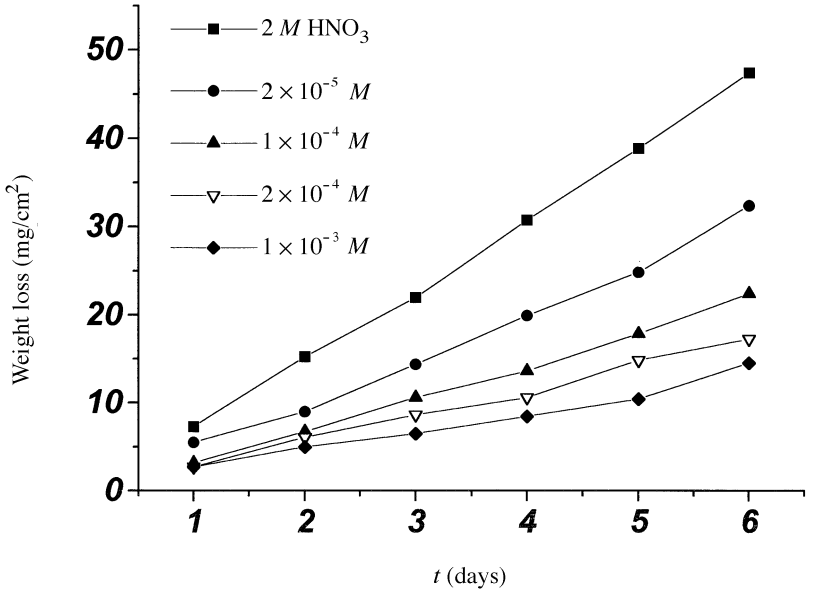

Fig. 8. Weight loss *vs* time curves of copper in 2 *M* HNO_3

ing inhibitor concentration. The adsorption of the inhibitor on the surface of the metal takes place through the lone pair electrons on the amino and pyridine nitrogen atoms; the presence of the hydroxy group favours the possibility of adsorption. The polarization data (Tables 2 and 3) show that 2-amino-3-hydroxypyridine acts as a mixed type inhibitor.

Table 4. Weight loss (mg/cm^2) for aluminum in 2 *M* HCl at different concentrations of 2-amino-3-hydroxypyridine at 303 K

Time (days)	0.0	2×10^{-5} *M*	1×10^{-4} *M*	2×10^{-4} *M*	1×10^{-3} *M*
1	28.7	15.9	13.7	7.9	5.2
2	75.4	35.7	24.5	16.1	11.5
3	125.6	60.0	40.4	26.3	18.1
4	179.7	87.8	59.6	36.4	27.0
5	245.8	116.2	71.3	43.8	33.7
6	297.2	181.6	80.9	50.8	36.6

Table 5. Weight loss (mg/cm^2) for copper in 2 *M* HNO_3 at different concentrations of 2-amino-3-hydroxypyridine at 303 K

Time (days)	0.0	2×10^{-5} *M*	1×10^{-4} *M*	2×10^{-4} *M*	1×10^{-3} *M*
1	7.2	4.1	3.1	2.1	2.0
2	15.2	9.0	7.0	6.0	4.9
3	21.9	14.3	10.5	8.7	6.5
4	30.3	19.9	13.5	10.5	8.3
5	38.8	24.8	17.7	14.7	10.3
6	47.2	32.4	22.4	17.4	13.2

Experimental

2-Amino-3-hydroxypyridine was bought from Aldrich and used without further purification; $ReO_2(PPh_3)_2I$ was synthesized by the literature method [37].

cis-$Mo_2O_5(ahp)_2 \cdot 3H_2O$

Ammonium molybdate $(NH_4)_2[MoO_4]$ (0.23 g, 1 mmol) in water (5 cm^3) was added to an aqueous solution of 2-amino-3-hydroxypyridine (0.11 g, 1 mmol). A yellow solution was obtained which was left at room temperature for one hour. The yellow precipitate was filtered off, washed with water and methanol, and air dried.

trans-$UO_2(ahp)_2$

Uranyl acetate dihydrate $U(CH_3COO)_2 \cdot 2H_2O$ (0.21 g, 0.5 mmol) in methanol (5 cm^3) was added to a solution of 2-amino-3-hydroxypyridine (0.11 g, 1 mmol) in methanol-water (10 cm^3, 2:1). The orange mixture was refluxed for two hours on a steam bath. The orange precipitate was filtered, washed with methanol and ether, and dried *in vacuo*.

$ReO(PPh_3)(ahp)_2I$

To a stirred suspension of $ReO_2(PPh_3)_2I$ (0.22 g, 0.25 mmol) in methanol (10 cm^3), 2-amino-3-hydroxypyridine (0.055 g, 0.5 mmol) was added. The resulting mixture was refluxed for two hours with stirring. The brown solution was filtered after cooling. After two days in the fridge, the shiny brown-green precipitate formed was filtered off, washed with cold methanol, and dried *in vacuo*.

$Ru(ahp)_3 \cdot 3H_2O$

Hydrated ruthenium chloride (0.13 g, 0.5 mmol) in methanol (10 cm^3) was added to 2-amino-3-hydroxypyridine (0.22 g, 2 mmol) in methanol (15 cm^3). The resulting mixture was refluxed for three hours, and a blue solution was obtained. The blue-black product formed upon reducing the volume to one half was filtered off and dried in a desicator over silica gel.

$Rh(ahp)_3 \cdot 4H_2O$

Hydrated rhodium trichloride (0.08 g, 0.25 mmol) was added to a solution of sodium acetate (0.2 g, 1.7 mmol) in water (15 cm^3) and 2-amino-3-hydroxypyridine (0.165 g, 1.5 mmol) with stirring. The yellow suspension was refluxed for two hours. The green precipitate formed was filtered while hot, washed with hot water, and dried on air.

$Fe(ahp)_3 \cdot 3H_2O$

To $FeCl_3 \cdot 6H_2O$ (0.27 g, 1 mmol) in water (10 cm^3), a solution of 2-amino-3-hydroxypyridine (0.33 g, 3 mmol) and NaOH (0.12 g, 3 mmol) in water (10 cm^3) was added. The dark brown solution was reduced to half of its volume, and the deep brown solid was filtered off, washed with water, and dried over silica gel.

$Pd(ahp)_2$

To an aqueous solution of $K_2[PdCl_4]$ (0.16 g, 0.5 mmol) 2-amino-3-hydroxypyridine (0.11 g, 1 mmol) was added. The suspension was stirred for five hours, and a yellow precipitate was obtained. It was filtered off, washed with water, and dried on air.

$Co(ahp)_2 \cdot 2H_2O$

Hydrated cobalt acetate (0.25 g, 1 mmol) in methanol (10 cm^3) was added to a solution of 2-amino-3-hydroxypyridine (0.22 g, 2 mmol) in methanol (10 cm^3). The reaction mixture was refluxed for two hours. The deep brown precipitate formed was filtered off, washed with methanol and ether, and dried *in vacuo*.

$Cu(ahp)_2$

A similar method to that for the preparation of $Co(ahp)_2 \cdot 2H_2O$ was used, replacing copper acetate by cobalt acetate.

Polarization and weight loss measurements

Cylindrical pieces of aluminum (99.54% purity) or copper (99.74% purity) were sealed to a glass tube with Araldite and used as electrodes in the galvanostatic polarization measurements. For weight loss measurements, sheet with dimensions $20 \times 20 \times 1$ mm were used. The metal surface was polished with emery paper, cleaned with distilled water, degreased [38, 39], washed with distilled water, and dried with filter paper. Analytical grade 2 *M* HCl (for aluminum) and 2 *M* HNO_3 (for copper) were used. Saturated calomel and platinium electrodes were used as reference and auxiliary electrodes, respectively. All experiments were performed at $30 \pm 0.2\,^{\circ}C$.

Instrumentation

Infrared spectra were measured as KBr discs on a Matson 5000 FTIR spectrometer. *Raman* spectra were recorded on a Perkin-Elmer 1760 X FT-IR instrument fitted with a 1700 X NIR-FT-*Raman* accessory (spectron Nd-YAG laser, 1064 nm excitation). Proton NMR spectra were measured on a Bruker WM-250 spectrometer. The magnetic susceptibilities were measured at room temperature on a Johnson Matthey magnetic susceptibility balance. The electronic spectra were measured on a Unicam UV2–100 UV/Vis spectrometer. Microanalyses were carried out by the Micro Analytical Unit, Cairo University, Egypt. Galvanostatic polarization measurements were carried out using an Amel potentiostat-549.

Acknowledgements

We thank Prof. *W. P. Griffith* for his advice and Mr. *P. Hammerton* for the ^{1}H NMR measurements. We thank the *University of London Intercollegiate Research Service* and Mr. *S. Bastians* for recording the *Raman* spectra at the Imperial College, London.

References

[1] Griffith WP, Koh TY, Williams DJ (1993) J Chem Soc Dalton Trans 3459
[2] Matsui H, Lever ABP, Auburn PR (1991) Inorg Chem **30**: 2402
[3] Flouzat C, Bresson Y, Mattio A, Bonnet J, Guillaumet G (1993) J Med Chem Bioorg **36**: 497
[4] Bansal SK, Tikku S, Sindhu RS (1991) J Ind Chem Soc **68**: 566
[5] El-Hendawy AM (1991) Polyhedron **10**: 2137
[6] Willet RD (1988) Acta Crystallogr Cryst Struct Commum **44C**: 450
[7] Mathur RP, Pradhan V, Mathur P (1993) Rev Roum Chem **38**: 1431
[8] Schmitt G (1984) Br Corros J **19**: 165
[9] Jmal MA, Mideren AS, Quraishi MA (1994) Corros Sci **36**: 79
[10] Fouda AF, Mahmoud AK (1990) J Electrochem Soc India **39**: 246
[11] Fouda AF, Mahmoud AK (1988) Werkst Korros **39**: 23
[12] Abd El-Maksoud SA, Shafei AA, Mostafa HA, Fouda AS (1995) Material and Corrosion **46**: 468
[13] Griffith WP, Mostafa SI (1992) Polyhedron **11**: 2997
[14] Griffith WP (1969) J Chem Soc A 211
[15] Griffith WP, Pumphrey CA, Rainey TA (1986) J Chem Soc Dalton Trans 1125
[16] El-Hendawy AM, El-Kourashy A, Shanab MM (1992) Polyhedron **11**: 523
[17] Edwards CF, Griffith WP, White AJ, Williams DJ (1992) J Chem Soc Dalton Trans 957
[18] Hingorani S, Singh K, Agarwala BV (1994) J Ind Chem Soc **71**: 183
[19] Leovac VM, Jovanovic LS, Bjelica LJ, Cesljevic VI (1989) Polyhedron **8**:135
[20] Rana VB, Sahni SK, Gupta SP, Sangal SK (1977) J Inorg Nucl Chem **39**: 1098
[21] Siddiqi ZA, Qidwai SN, Mathew VJ (1993) Synth React Inorg Met-Org Chem **23**: 709
[22] AcArdle JV, Sofen RS, Cooper RS, Raymond KN (1978) Inorg Chem **17**: 3075
[23] Dengel AC, Griffith WP, Powell RD, Skapski AC (1987) J Chem Soc Dalton Trans 991
[24] Griffith WP, Pumphrey CA, Skapski AC (1989) Polyhedron **8**: 2813
[25] Griffith WP, Nogueria HIS, Parkin BC, Sheppard RN, White AJP, Williams DJ (1995) J Chem Soc Dalton Trans 1775
[26] Prabhakar B, Reddy KL, Lingaiah P (1988) Ind J Chem **27A**: 217
[27] El-Asmy AA, Mounir M (1988) Trans Met Chem **13**: 143
[28] Jorgensen CK (1962) J Inorg Nucl Chem **24**: 1521
[29] Satpathy KC, Mishra R, Jal BB (1986) J Ind Chem Soc **LXIII**: 377
[30] Rajaram V, Ramalingam SK (1984) Trans Met Chem **9**: 48
[31] Sacconi L, Ciampolini M (1964) J Chem Soc 276

[32] Kato M, Jonassen MB, Fanning JC (1964) Chem Rev **64**: 99
[33] Fung KW, Johnson KE (1971) Inorg Chem **10**: 1347
[34] Figgis BN, Lewis J (1960) In: Lewis J, Wilkins RC (eds) Modern Coordination Chemistry. Interscience, New York
[35] Sangri HS, Sodhi GS, (1990) Ind J Chem **29**: 922
[36] Casey AT, Vecchio AM (1988) J Coord Chem **16**: 375
[37] Ciani GF, D'Alfonso G, Romiti PF, Sironi A, Freni M (1983) Inorg Chim Acta **72**: 29
[38] Kim CP, Nobe K (1971) Corrosion-NACE **27**: 382
[39] Aziz K, Shams El-Din AM (1965) Corros Sci **5**: 489

Received July 24, 1997. Accepted (revised) September 10, 1997